Microstructural evolution and the role of interfaces in Mg–Zn–Y alloys with high strength and formability

2008 J. Phys.: Condens. Matter 20 314001

(http://iopscience.iop.org/0953-8984/20/31/314001)

J. Phys.: Condens. Matter **20** (2008) 314001 (10pp) doi:10.1088/0953-8984/20/31/314001

Microstructural evolution and the role of interfaces in Mg–Zn–Y alloys with high strength and formability

H J Chang[1], J Y Lee[2] and D H Kim[2]

[1] Division of Humantronics Information Materials, Yonsei University, 134 Shinchondong, Seodaemungu, Seoul 120-749, Korea
[2] Department of Materials Science and Engineering, Center for Non-crystalline Materials, Yonsei University, 134 Shinchondong, Seodaemungu, Seoul 120-749, Korea

E-mail: dohkim@yonsei.ac.kr

Received 16 May 2008
Published 11 July 2008
Online at stacks.iop.org/JPhysCM/20/314001

Abstract
Composites consisting of a quasicrystalline, icosahedral phase (I-phase) and ductile α-Mg can be fabricated by controlling the alloy composition in the Mg–Zn–Y alloy system. The I-phase in Mg–Zn–Y alloys shows a variation in structural order from a well-ordered icosahedral phase to a 1/1 rhombohedral approximant phase. The structural change in the icosahedral phase can be explained by microdomain formation due to compositional change during solidification. The characteristic of strong bonding between icosahedral particles and the α-Mg matrix indicates that the structural change from I-phase to crystalline phase is not discontinuous, but gradual. The interface layer of α-Mg with several nm thickness preserves an orientational relationship with the I-phase, although the remaining α-Mg shows a different orientation due to plastic deformation during deformation (rolling process). Such a strong interface can provide an excellent combination of high strength and formability in Mg-based alloys, enabling application as lightweight structural parts.

1. Introduction

Thermally stable icosahedral phases (I-phases) have been reported to form in several alloy systems including Al–Cu–Fe and Zn–Mg–Y. In these alloy systems, *in situ* composites may be prepared by controlling the alloy composition and the solidification process. For ease in controlling microstructure and optimizing process parameters, it is preferable to have a wide two-phase region, consisting of I-phase and crystalline phase. In the case of the Al–Cu–Fe system, there are several two-phase regions where the I-phase coexists in equilibrium with another phase [1]. However, the compositional range of the two-phase region is very limited and all the coexisting phases are brittle. Therefore, fabrication *in situ* of composite materials in the Al–Cu–Fe system may not be promising from an engineering point of view.

In the case of Zn–Mg–Y, a thermodynamically stable I-phase has been reported to form with composition of about $Mg_{42}Zn_{50}Y_8$ (in at.%) [2, 3]. The process of formation of I-phase in the Zn–Mg–Y system has been studied in detail by Tsai *et al* in alloys with more than 50 at.% Zn [4]. They have shown that the I-phase forms by a peritectic reaction between previously formed $(Zn, Mg)_5Y$ and residual Mg-enriched liquid phase, during solidification from the alloy melt. Langsdorf *et al* have shown that there is a wide compositional range for I-phase formation as a primary phase in the Mg–Zn–Y system, while Luo *et al* have observed a eutectic-like structure consisting of α-Mg and I-phase near the grain boundaries in Mg-rich Mg–Zn–Y alloys [5, 6]. These experimental observations suggest that a two-phase region (I-phase + α-Mg) exists in the Mg-rich Mg–Zn–Y ternary system. Indeed Tsai *et al* have suggested a two-phase region towards the Mg-rich corner of the Mg–Zn–Y phase diagram as shown in figure 1 [7].

The existence of the two-phase region, I-phase + α-Mg phase, in the Mg-rich corner of the Mg–Zn–Y system indicates that small additions of Y in the binary Mg–Zn system can change the alloy microstructure significantly. The primary dendrite in the binary alloy $Mg_{74}Zn_{26}$ is the α-Mg phase, while the I-phase exists as the primary phase

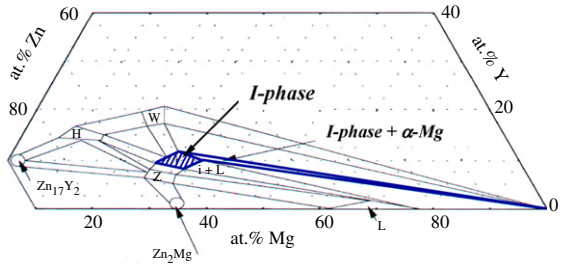

Figure 1. A Mg–Zn–Y ternary phase diagram for the isothermal section of 700 K [7].

(This figure is in colour only in the electronic version)

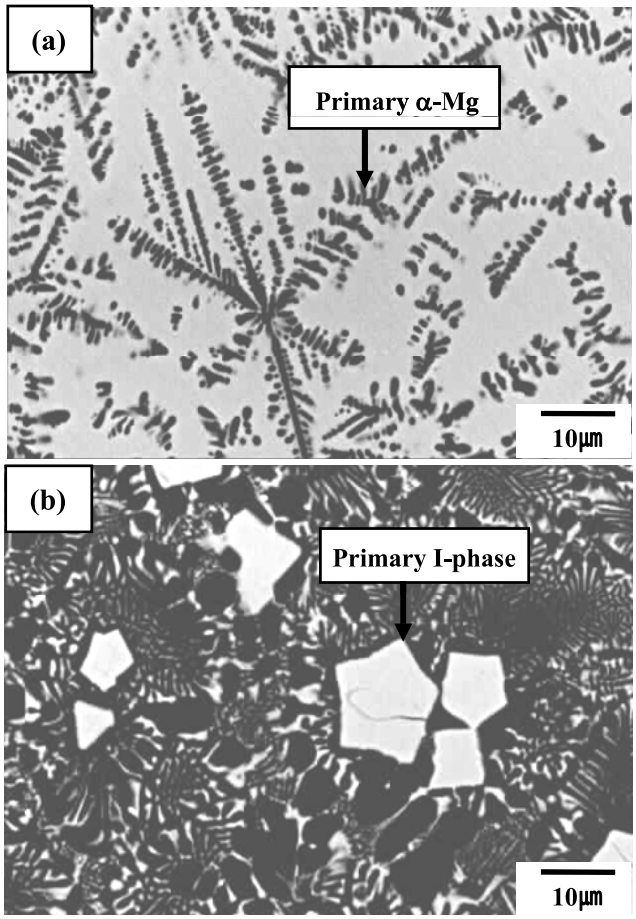

Figure 2. Backscattered images in SEM of the as-cast alloys; (a) $Mg_{74}Zn_{26}$ alloy and (b) $Mg_{72.5}Zn_{25.5}Y_2$ alloy [8].

in the alloy $Mg_{72.5}Zn_{25.5}Y_2$ as shown in figures 2(a) and (b) [8]. The primary I-phase is enveloped in a lamellar colony, indicating that there is a pseudobinary eutectic reaction between the I-phase and α-Mg phase. A detailed study on the formation of the I-phase has shown that as-cast Mg-rich Mg–Zn–Y alloys in the compositional range up to the pseudo-eutectic composition of $Mg_{73.2}Zn_{23}Y_{3.8}$ (where the ratio of Zn to Y is around 6) consist of the thermally stable I-phase formed *in situ* as a second phase in the α-Mg matrix during solidification, indicating that I-phase reinforced Mg composites can be fabricated just by

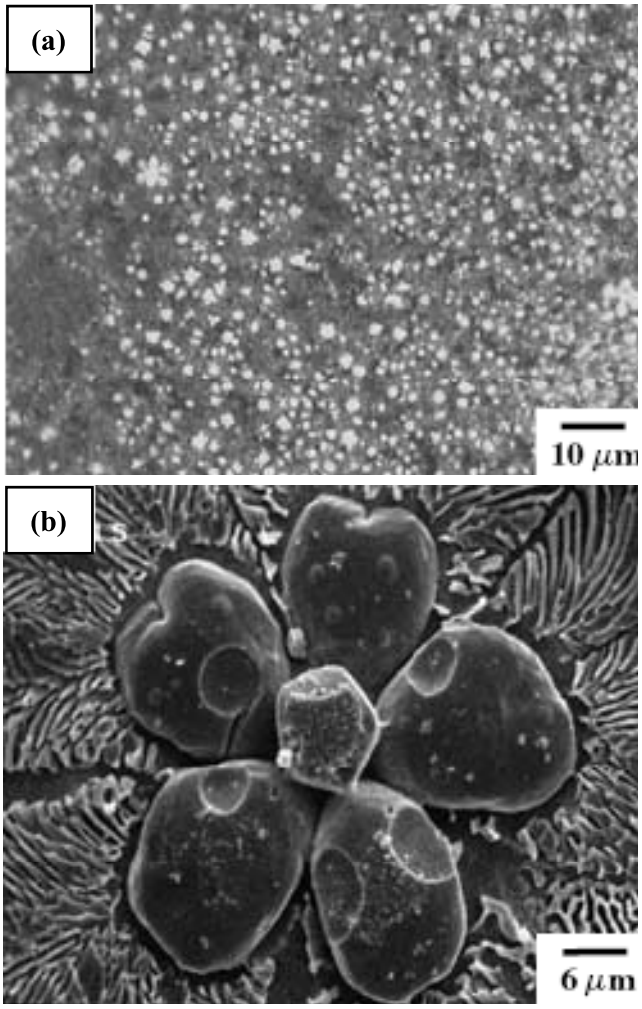

Figure 3. Typical microstructures of as-cast $Mg_{68}Zn_{28}Y_4$ alloy: (a) optical micrograph and (b) scanning electron micrograph [9].

solidification from the alloy melt [9]. In this paper, the microstructure evolution in the as-cast and deformed Mg–Zn–Y alloy system reported so far has been reviewed, with a special emphasis on the role of the interface in enhancing the mechanical properties.

2. Evolution of microstructure in as-cast Mg–Zn–Y alloy

Figure 3 [9] shows typical optical and scanning electron micrographs, obtained from an as-cast lower Mg content $Mg_{68}Zn_{28}Y_4$ ingot. The alloy microstructure consists of randomly distributed primary solidification phase embedded in a lamellar eutectic structure formed at a later stage of solidification with a transient region between the primary and eutectic regions. The primary crystals show a dendritic morphology with several lateral branches. The number of branches varies, depending on the orientation of the cross section. However, some of the dendrites show five lateral branches as shown in figure 3(b), indicating clearly the fivefold anisotropy characteristic of icosahedral quasicrystalline phase. The energy of the interface between I-phase and liquid is small

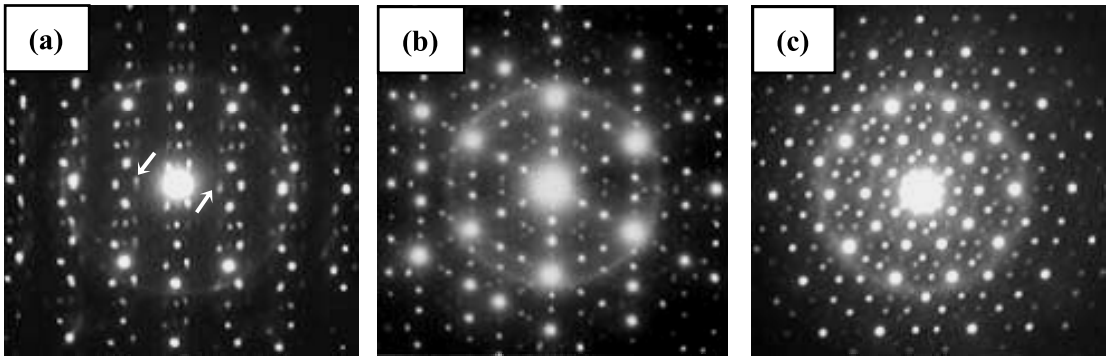

Figure 4. Selected-area diffraction patterns (SADPs) taken from the primary I-phase of the as-cast $Mg_{68}Zn_{28}Y_4$ alloy [9].

Table 1. Nominal alloy compositions and constituent phases in the as-cast samples identified via x-ray diffraction.

Group	Alloy No.	Composition (at.%) Mg	Zn	Y	Zn/Y ratio	Vol. fraction of interdendritic region (%)	Phase
A	1	98.36	1.53	0.11	13.60	—	α-Mg + Mg_7Zn_3
	2	96.62	3.15	0.23	13.70	—	
B	3	98.72	1.14	0.14	8.16	1.2	α-Mg + I-phase
	4	98.69	1.14	0.17	6.80	1.2	
	5	98.30	1.53	0.17	9.00	2.2	
	6	98.24	1.53	0.23	6.80	2.3	
	7	97.32	2.34	0.34	6.80	2.9	
	8	96.36	3.17	0.47	6.80	3.7	
	9	95.00	4.3	0.7	6.14	5.1	
C	10	98.52	1.15	0.34	3.40	1.2	α-Mg + I-phase + W-phase
	11	98.00	1.54	0.45	3.40	2.4	
	12	97.88	1.55	0.57	2.72	2.6	
	13	97.12	2.16	0.72	3.00	2.9	
D	14	98.40	1.15	0.45	2.55	—	α-Mg + W-phase
	15	97.82	1.55	0.63	2.47	—	

due to a structural similarity of the two phases [10]. Therefore, the stabilization of the planar solid/liquid (S/L) interface by the interface energy contribution is not expected to be strong and dendrites develop at an early stage of growth. The pattern of dendrites is strongly dependent on the anisotropy of growing crystal. Due to the fivefold symmetry of the I-phase, five lateral branches appear during dendritic growth as shown in figure 3(b).

Figure 4 shows selected-area diffraction patterns (SADPs) taken from the primary solidification phase, corresponding to twofold, threefold and fivefold rotation symmetries of primitive-type (P-type) icosahedral quasicrystalline phase in the as-cast $Mg_{68}Zn_{28}Y_4$ alloy [9]. The patterns also indicate that the I-phase does not show a perfect icosahedral quasicrystalline structure. The presence of phason strain can be inferred from the shift of diffraction spots from their ideal positions as marked by arrows.

With increasing Mg content (i.e. in higher Mg content alloy), the primary solidification phase changes from I-phase to dendritic α-Mg phase, and a eutectic structure with lamellar spacing of about 100 nm can be obtained in the interdendritic region [9]. Higher content of Mg makes α-Mg phase nucleate first and grow into a dendrite, and at a later stage of solidification the remaining liquid in interdendritic regions solidifies into a eutectic structure consisting of I-phase (or Mg_7Zn_3, $Mg_3Zn_3Y_2$ phases) and α-Mg phase, depending on the alloy composition. The typical two-phase or three-phase regions surrounding the I-phase + α-Mg two-phase region in the higher range of Mg composition are listed in table 1. The phase regions are classified into four groups based on the Zn/Y ratios [11]. As described in table 1, A, B, C and D groups include the alloy compositions with Zn/Y ratios of ∼13, 6–9, 2.7–3.4 and 2.4–2.6, respectively, illustrating that phases in the as-cast microstructure differ depending on the Zn/Y ratio. The characteristics of the four groups, A–D, are: A group (Zn/Y ratio ∼13), α-Mg + Mg_7Zn_3 (cubic, $a = 1.417$ nm); B group (Zn/Y ratio 6–9), α-Mg + I-phase; C group (Zn/Y ratio 2.7–3.4), α-Mg + I-phase + W-phase ($Mg_3Zn_3Y_2$; cubic, $a = 0.683$ nm [12]); and D group (Zn/Y ratio: 2.4–2.6), α-Mg + W-phase. This shows clearly that the formation of the interdendritic second phase is strongly dependent on the Zn/Y ratio. Higher Zn/Y ratio (∼13) favors the formation the Mg_7Zn_3 phase since the composition becomes close to the binary Mg–Zn system. As the Zn/Y ratio decreases (6–9), the I-phase replaces the Mg_7Zn_3 phase in the interdendritic region. The Mg_7Zn_3 phase has been reported as a 1/1 cubic approximant of I-phase in the Mg–Zn–Y alloy system by Luo *et al* [12], indicating that there is a structural relationship

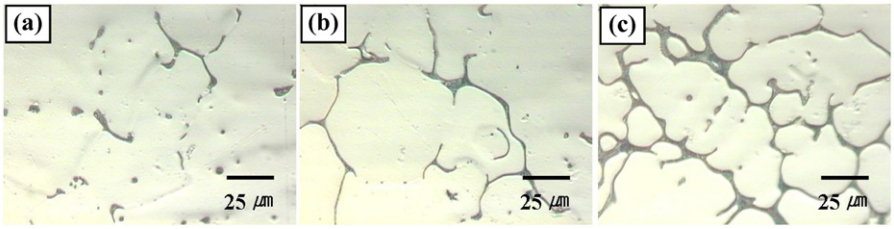

Figure 5. Optical micrographs of the as-cast alloys: (a) $Mg_{98.69}Zn_{1.14}Y_{0.17}$ alloy; (b) $Mg_{98.24}Zn_{1.53}Y_{0.23}$ alloy and (c) $Mg_{96.36}Zn_{3.17}Y_{0.47}$ alloy.

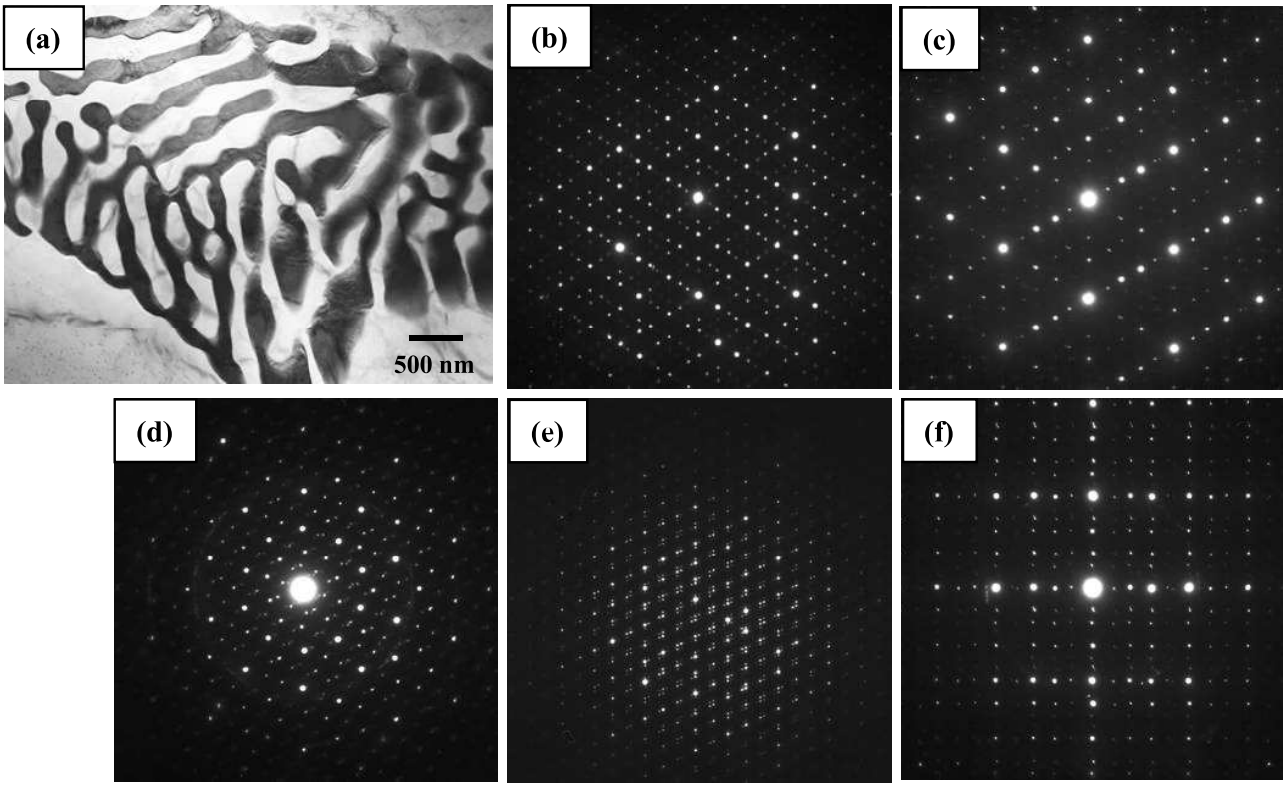

Figure 6. (a) TEM BF image of the interdendritic region; ((b)–(f)) SADPs obtained from eutectic phase corresponding to twofold, threefold, fivefold and two different types of pseudo-twofold symmetries of I-phase of as-cast $Mg_{91.5}Zn_{7.8}Y_{0.7}$ alloy.

between I-phases and Mg_7Zn_3 phases. As the Zn/Y ratio decreases further (2.7–3.4), the W-phase begins to form in the interdendritic region. The optimum Zn/Y ratio for forming the I-phase reinforced composite of the Mg–Zn–Y system is 6–9.

Figures 5(a)–(c) show the optical microstructures of the as-cast $Mg_{98.69}Zn_{1.14}Y_{0.17}$ alloy, $Mg_{98.24}Zn_{1.53}Y_{0.23}$ alloy and $Mg_{96.36}Zn_{3.17}Y_{0.47}$ alloy in the B group in table 1. The fraction of the interdendritic eutectic increases with increasing zinc and yttrium contents. The volume fraction of the interdendritic eutectic region measured using an image analyzer is 1.2, 2.3 and 3.7% in $Mg_{98.69}Zn_{1.14}Y_{0.17}$ alloy, $Mg_{98.24}Zn_{1.53}Y_{0.23}$ alloy and $Mg_{96.36}Zn_{3.17}Y_{0.47}$ alloy, respectively, as shown in table 1.

Figure 6(a) shows the typical TEM images of the interdendritic regions of the as-cast $Mg_{91.5}Zn_{7.8}Y_{0.7}$ alloy. The SADPs (figures 6(b)–(f)) taken from the eutectic phase correspond to twofold, threefold, fivefold and two different types of pseudo-twofold symmetries of an I-phase which is different from that observed in low Mg content alloys (figure 4). The patterns show that the I-phase corresponds to a face-centered (F-type) six-dimensional hypercubic lattice as in the Al–Cu–Fe alloy. In addition to the eutectic structure of I-phases and α-Mg phases, fine polygon-shaped I-particles (20–30 nm) are distributed in the α-Mg matrix, as shown in figure 7(a). The I-particles are somewhat aligned. This implies that they form in the liquid state, and then are included in the α-Mg grain ahead of the S/L interface during solidification. The projected morphologies of the I-phase particles and schematic drawings of a pentagonal dodecahedron, which is projected along its fivefold, threefold and twofold symmetry axes, are shown in figures 7(b)–(d). The polygonal shapes again show that the I-phase particles formed directly from the melt. These types of morphologies of the I-phase have been reported to form directly from the melt as primary particles in Al–Mn alloys [13].

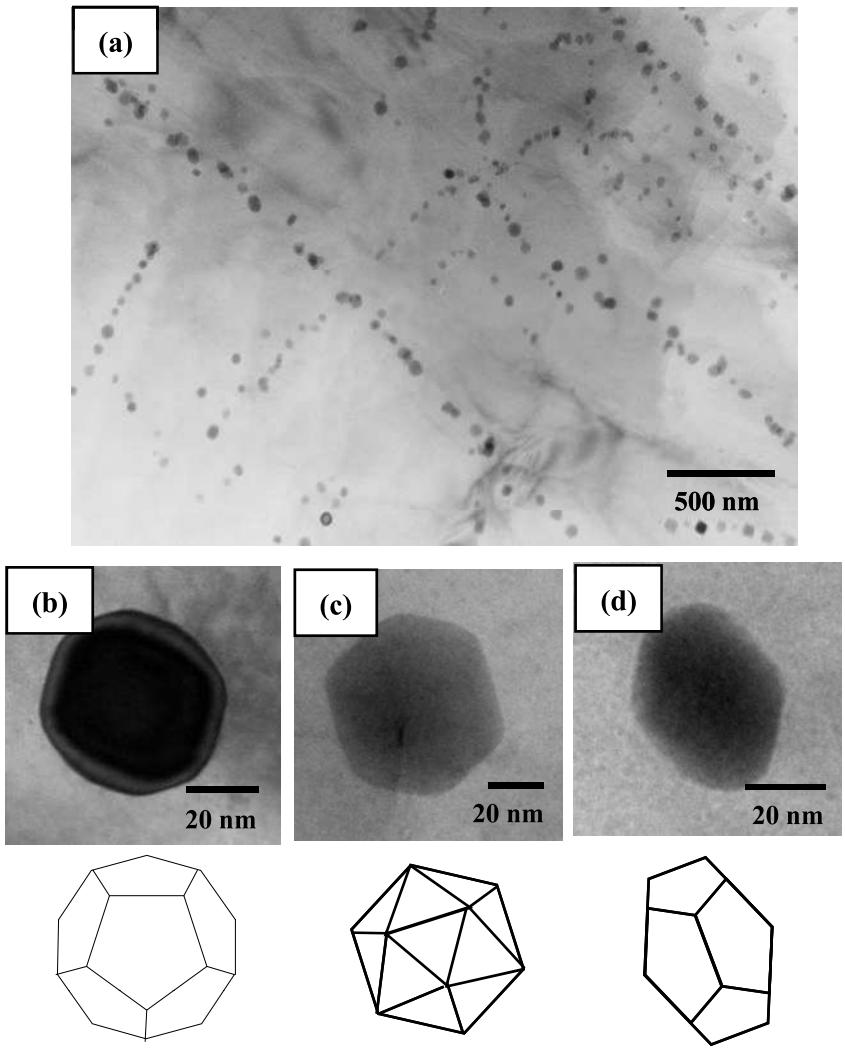

Figure 7. (a) TEM BF image of nanoicosahedral particles in the α-Mg matrix of as-cast $Mg_{91}Zn_{8.3}Y_{0.7}$ alloy; ((b)–(d)) the projected morphologies of the I-particles and the corresponding schematic drawings of pentagonal dodecahedron, which is projected along its fivefold, threefold and twofold symmetry axes, respectively.

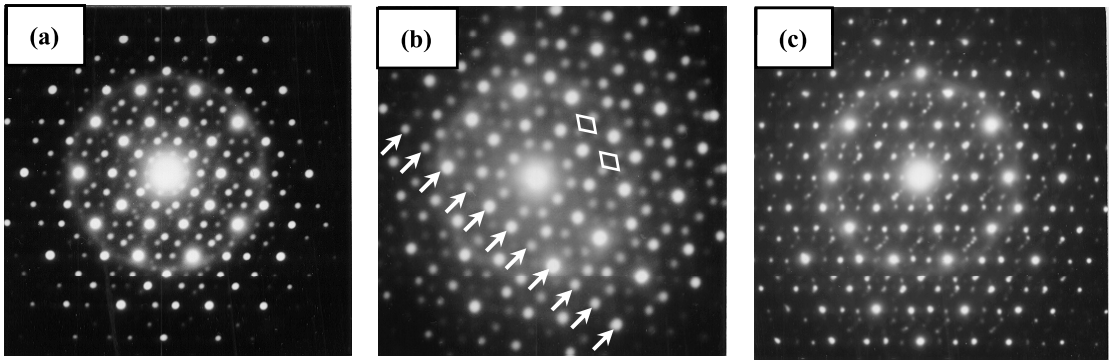

Figure 8. SADPs taken from three different parts within a primary I-phase without tilting the specimen during observation: ((a), (b)) with an aperture of 0.1 mm diameter; (c) with an aperture of 0.5 mm diameter [9].

3. Inhomogeneous structural order in I-phase and the approximant

Although well-ordered icosahedral quasicrystalline patterns can be taken in some parts of the primary phase, the degree of structural order in the I-phase varies depending on the position even within a single grain in low Mg content alloys. An example is shown in figure 8. Comparing with the SADP in figure 4(c), decagons surrounding the transmitted beam

are significantly distorted, indicating that structural perfection in this region is low. Indeed the diffraction spots along a certain direction are rather regularly spaced as marked by arrows. The deviation of the diffraction pattern from the ideal icosahedral fivefold diffraction pattern also can be noted from the marked rhombus, instead of pentagon formation between the second and third distorted decagons. In fact, the diffraction pattern may be considered to show a periodic array of the rhombus, which is a characteristic of an ordinary crystalline phase. However, the strong spots show characteristics of a quasicrystalline phase such as aperiodic distribution in the form of pentagons or decagons.

The SADPs in figures 9(a) and (b) consist of regularly spaced periodic diffraction spots, which can be indexed as [110] and [010] zone diffraction patterns, respectively, of a rhombohedral phase with lattice parameters of $a = 27.2$ Å and $\alpha = 63.43°$, as shown in figures 9(c) and (d). The tilting angle between two zones was about 32°, which is close to the value of 31.7° calculated from the rhombohedral structure. However, it can be noticed that distributions of the strong diffraction spots (marked by small circles) in the patterns of figures 9(a) and (b) closely resemble corresponding distributions in diffraction patterns taken from I-phase with the incident beam axis parallel to a twofold axis and a fivefold axis, respectively. Diffraction spots with strong intensity are not regularly spaced, as in the diffraction patterns of the quasicrystalline phase (figure 8). Therefore, the rhombohedral phase can be considered as an approximant phase for the icosahedral quasicrystalline phase in the Mg–Zn–Y system. Local formation of rhombohedral micrograins or microdomains in the icosahedral structure is likely because there is a group–subgroup relation between the icosahedral and the rhombohedral structures. Rhombohedral microdomains in icosahedral crystal have also been observed in the Al–Cu–Fe system [14]. Two different types of rhombohedral approximants have been reported in Al–Cu–Fe alloys: a 2/1 approximant with $a = 37.7$ Å and $\alpha = 63.43°$; a 3/2 approximant with $a = 61.0$ Å and $\alpha = 63.43°$. The lattice parameter of a rhombohedral q/p approximant can be expressed as follows [15]:

$$a = 2(p + q\tau)a_{\mathrm{R}},$$

where τ and a_{R} are the golden mean and the smallest rhombohedron edge length of the icosahedral quasicrystal, respectively. By using the reported value of $a_{\mathrm{R}} = 5.2$ Å for the MgZnY icosahedral quasicrystal [16], the lattice constant of the 1/1 rhombohedral approximant is expected to have $a = 2(1 + \tau)a_{\mathrm{R}} = 27.2$ Å. When compared with the pseudo-twofold diffraction patterns of the 2/1 and 3/2 rhombohedral approximants reported by Liu *et al* [14], the approximant phase in the Mg–Zn–Y system can be identified as the 1/1 rhombohedral approximant [9].

The gradual change in structural order or the presence of intermediate structure between rhombohedral and icosahedral structures can be explained by the formation of microdomain structure with specific orientation of rhombohedra as in the Al–Cu–Fe system [14]. The formation of microdomains may be related to the compositional change in the I-phase. It has been reported that the I-phase composition shifts towards the Mg-rich side as temperature decreases [7]. Therefore it is expected that variation in composition exists within the I-phase due to a rather long temperature range of pseudo-eutectic solidification. Also, the solidification process is not an equilibrium process. Due to capillary effects, local change in composition is also expected. The composition of the rhombohedral phase, measured by energy dispersive x-ray spectroscopy, is in the range of $ZnMg_{(35-40)}Y_{(7-9)}$. The composition is not very different from the previously reported I-phase composition of $Zn_{50}Mg_{42}Y_8$ [16].

The improvement of structural order in icosahedral structure results from homogenization, supporting the idea that the I-phase is indeed a thermodynamically stable phase, and structural disorder of the I-phase in as-cast specimens is related to variation of composition. A TEM study reveals that the 1/1 rhombohedral approximant is metastable and changes into the I-phase during annealing. The diffraction pattern obtained from a specimen annealed for 100 h at 350 °C exhibits well-ordered fivefold rotational symmetry [9]. The sharp reflections and well-ordered pentagon and decagons indicate that the I-phase exhibits a highly ordered structure.

4. Evolution of microstructure after deformation

Alloy ingots were hot rolled from an initial thickness of 10 mm to a final thickness of 1.0 mm with a rolling speed of 6.4 mm s^{-1}. The total reduction ratio was 90%. The rolling process started with a reduction ratio of 10% and ended with a reduction ratio of 30%. The roll was heated to around 100° prior to rolling. Before rolling, the samples were heated at 400° for 15 min. The as-cast eutectic structure in the dendritic region was destroyed during the hot rolling process, providing the distribution of I-particles (0.3–2.0 μm in size) shown in figures 10(a) and (c). The existence of an I-phase in the deformed specimen clearly indicates that the I-phase thermally equilibrates with the α-Mg phase. A relatively fine grain size can be obtained due to the dynamic recrystallization (DRX) process during thermomechanical processing. The cracked I-particles effectively act as dynamic recrystallization sources during hot rolling, helping to refine the grains of the α-Mg matrix (figure 10(b)). TEM observation revealed that the size of the pre-existing I-particles did not change significantly (~100 nm) even after long exposure at high temperature, i.e. homogenization (400° for 12 h), and rolling/annealing (430° for 1 h) (figure 10(c)). Kim *et al* have shown that the I-particles do not coarsen significantly at high temperature, inhibiting grain growth during deformation at high temperatures [17]. There are two reasons for the negligible coarsening of the I-particles. First, considering that the atomic size of Y is 12% larger than the size of Mg, low diffusivity of Y in the α-Mg matrix is expected. Second, the interfacial energy of the quasicrystalline precipitate is lower than that of some intermetallic compounds developed in other Mg alloys due to the characteristic of strong bonding between the quasicrystalline phase and the α-Mg matrix, as shown in [18].

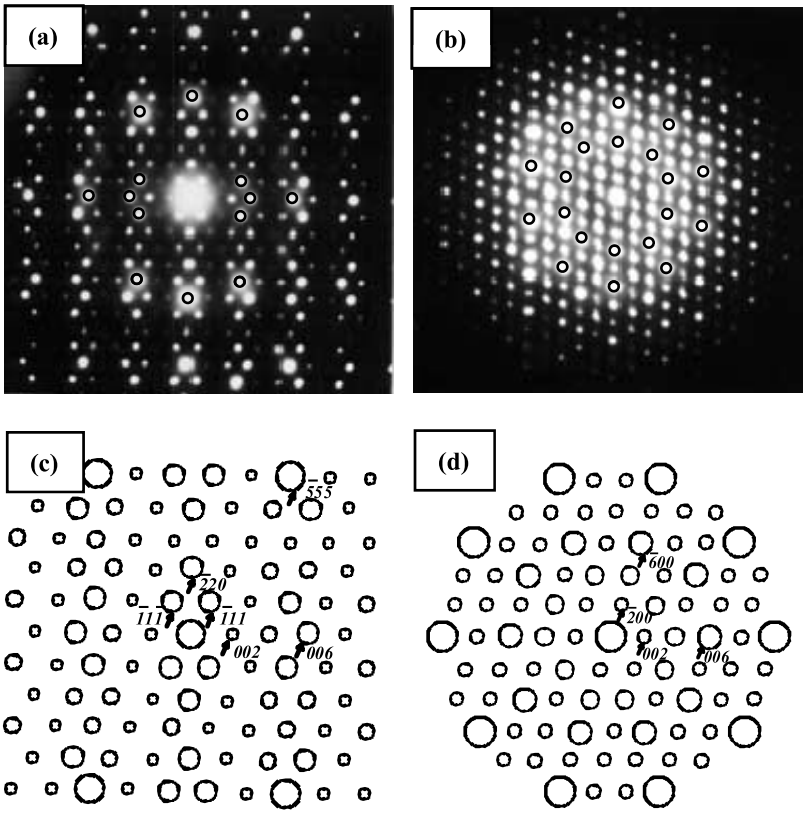

Figure 9. ((a), (b)) SADPs taken from part of the primary phase, obtained by tilting the specimen during TEM observation; ((c), (d)) corresponding schematic diagrams with analyzed results of the SADPs.

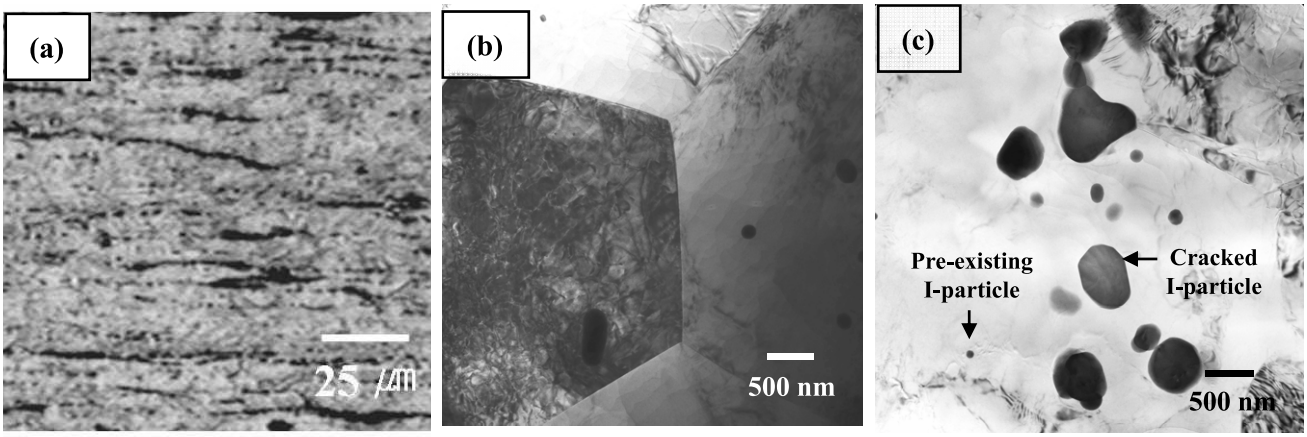

Figure 10. (a) Optical micrograph of the as-rolled alloys $Mg_{98.24}Zn_{1.53}Y_{0.23}$ alloy; TEM BF images showing (b) the refined α-Mg grain and (c) destroyed icosahedral particles (0.3–2 μm) and pre-existing icosahedral particles ($\sim$100 nm).

5. Interface between I-phase and Mg matrix

In most alloys containing second-phase particles, the cavities at the matrix/particle interface emerge and grow during the deformation. The cavity nucleation is known as matrix/particle decohesion, possibly starting from interfacial defects. Debonding between particle and matrix can occur during rolling processes. Thus, the rolling process leaves defects (weakly bonded interfaces or broken particles) in the material, and they do not generally self-sinter fully even after an exposure at high homologous temperature.

However, no cavities have been detected in deformed quasicrystalline particle reinforced Mg–Zn–Y alloy. The characteristic of strong bonding between icosahedral particles and α-Mg matrix is explained by high resolution electron microscopy (HREM) observations (figure 11). The image is obtained when the electron beam is parallel to the icosahedral twofold axis, but not to a high symmetry axis of the Mg matrix. Due to no apparent orientation relationship after the deformation and the lattice mismatch, the lattice fringes at the interface are not continuous. (The orientation relationship and the property of the interface between crystal and quasicrystal

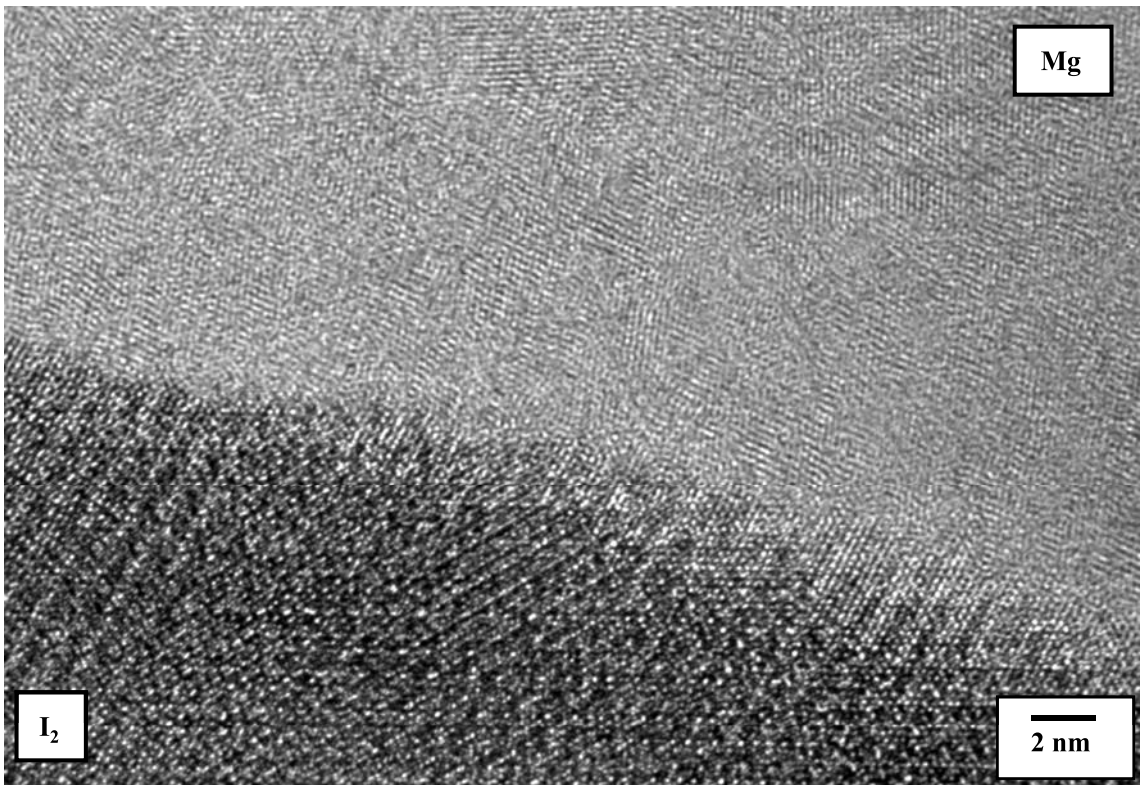

Figure 11. High resolution TEM image which was obtained from the interface between cracked eutectic I-particles and the matrix when the icosahedral twofold axis was parallel to the electron beam.

before mechanical deformation are shown in reference [20].) However, along the interface between the I-phase particle and α-Mg matrix, intermediate lattice fringes with a 1–2 nm thickness stemming from the I-phase are observed. This suggests that the structural change from I-phase to crystalline phase is not discontinuous, but gradual. Since the I-phase exhibits a more isotropic character than the crystalline phase due to its highly symmetric structure, reasonably stable bonding with low strain energy in the matrix adjacent to the I-phase particle can be provided. In general, the matrix adjacent to the microscale intermetallic particle is highly stressed due to the lattice constant mismatch between the matrix and the particle. However, due to the quasiperiodic lattice structure of the I-phase, the mismatch strain may be compensated by the I-phase particle, decreasing the stress concentration in the matrix near the I-phase particle.

Figure 12(a) shows the HREM micrograph of the interface region, between an I-phase particle and α-Mg matrix in Mg–Zn–Y alloy (hot rolled and annealed) [17]. It also shows the characteristic of strong bonding between I-phase and α-Mg matrix with no cavitations at the interface. The FT pattern in figure 12(d) obtained from the interface region of the α-Mg matrix shows a [0001] zone of the hexagonal structure. Due to the reflection from outside the region oriented along the hexagonal axis, additional $(10\bar{1}0)$ diffraction spots marked in figure 12(d) are also present. However, as marked in the high resolution TEM image, a hexagonal array of the lattice fringe is clearly observed along the interface region of the α-Mg matrix. Superposition of the FT patterns in figures 12(b) and (d) shows an orientation relationship of [I2] ∥ [0001]Mg, 2f and 5f (marked by ∗ in figure 12(d)) ∥ $\{10\bar{1}0\}$Mg with a slight misorientation (∼2°) which can be observed between $(10\bar{1}0)$ and (2f) in the high resolution TEM image. The same type of orientational relationship has been reported for Mg–Cd–Yb alloys, with the hexagonal [0001] axis of Mg parallel to one of the [I2] axes of the icosahedral phase [20]. The HREM analysis indicates that the interface layer of α-Mg with 3–5 nm thickness still preserves the orientation relationship with the I-phase, although the remaining α-Mg shows a different orientation due to plastic deformation during rolling. This coherency of the I-phase and α-Mg may be achieved by introducing steps or ledges periodically along the interface. Atomic scale bonding between the I-phase and the hexagonal structure is rigid enough to be retained during severe plastic deformation [17].

6. Summary and application of Mg–Zn–Y alloy

Composites consisting of I-phase and ductile α-Mg can be fabricated by controlling alloy composition. With increasing Mg content, the primary solidification phase changes from I-phase to α-Mg phase, and a single eutectic structure can be obtained at a composition of $Mg_{72}Zn_{23.5}Y_{3.5}$. The I-phase shows a variation in structural order from a well-ordered icosahedral phase to a 1/1 rhombohedral approximant phase. The structural change in the icosahedral phase can be explained by microdomain formation due to compositional change during solidification. In rolled Mg–Zn–Y sheets, no cavity is observed

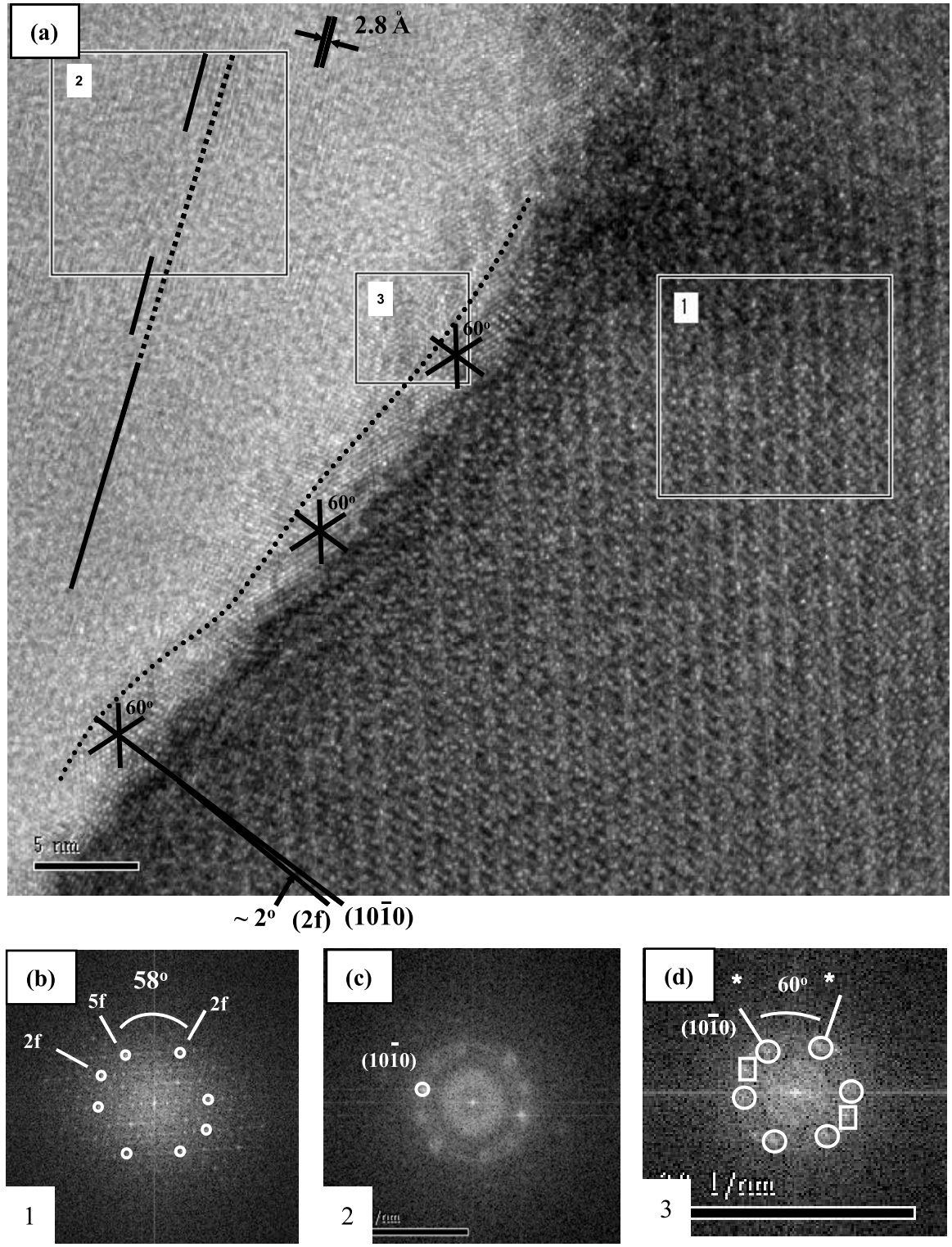

Figure 12. (a) High resolution TEM micrograph of the region of the interface between an I-phase particle and α-Mg matrix after hot rolling and annealing. The Fourier transformed (FT) patterns (b), (c), and (d) are obtained form the regions marked 1, 2, and 3, respectively, shown in (a). The image is obtained from the I-phase particle oriented along the twofold symmetry axis [I2] of the icosahedral symmetry [17].

at the interface. A characteristic of strong bonding between icosahedral particles and the α-Mg matrix is evidenced by HREM observations, showing that the structural change from I-phase to crystalline phase is not discontinuous, but gradual. The interface layer of α-Mg, which is several nm thick, still preserves the orientational relationship with the I-phase, although the remaining α-Mg shows a different orientation due to plastic deformation during rolling. Such a strong interface can provide an excellent combination of high strength and formability in Mg-based alloys. This can enable applications as

Figure 13. Micrograph of prototype sheet metal parts of the cellular phone case made by warm forming using quasicrystal strengthened Mg–Zn–Y alloys.

lightweight structural parts, for example as a part of the cellular phone case shown in figure 13.

Acknowledgments

This work was supported by the Fundamental R and D Program for Core Technology of Materials funded by the Korean Ministry of Commerce, Industry and Energy, the Global Research Laboratory Program funded by the Korean Ministry of Science and the Second Stage of Brain Korea 21 Project in the Division of Humantronics Information Materials.

References

[1] Gayle F W, Shapiro A J, Biancaniello F S and Boettinger W J 1992 *Metall. Mater. Trans.* A **23** 2409
[2] Tsai A P, Niikura A, Inoue A, Masumoto T, Nishita Y, Tsuda K and Tanaka M 1994 *Phil. Mag. Lett.* **70** 169
[3] Sato T J, Abe E and Tsai A P 1998 *Phil. Mag. Lett.* **77** 213
[4] Tsai A P, Niikura A, Inoue A and Masumoto T 1997 *J. Mater. Res.* **12** 1468
[5] Langsdort A, Ritter F and Assmus W 1997 *Phil. Mag. Lett.* **75** 381
[6] Luo Z P, Zhang S Q, Tang Y L and Zhao D S 1993 *Scr. Metall. Mater.* **28** 1513
[7] Tsai A P, Murakami Y and Niikura A 2000 *Phil. Mag.* A **80** 1043
[8] Yi S, Park E S, Ok J B, Kim W T and Kim D H 2001 *Mater. Sci. Eng.* A **300** 312
[9] Ok J B, Kim I J, Yi S, Kim W T and Kim D H 2003 *Phil. Mag.* **83** 2359
[10] Xu D K, Liu L, Xu Y B and Han E H 2006 *J. Alloys Compounds* **426** 155
[11] Lee J Y, Kim D H, Lim H K and Kim D H 2005 *Mater. Lett.* **59** 3801
[12] Luo Z P, Sui H X and Zhang S Q 1996 *Metall. Mater. Trans.* A **27** 1779
[13] Kim D H and Cantor B 1989 *Scr. Metall.* **23** 1859
[14] Liu W, Koster U and Zaluska A 1991 *Phys. Status Solidi* **125** K9
[15] Audier M and Guyot P 1990 *Quasicrystals and Incommensurate Structures in Condensed Matter* ed M J Yackaman, D Romeu, V Castano and A Gomez (Singapore: World Scientific) p 288
[16] Tsai A P, Niikura A, Inoue A, Masumoto T, Nishita Y, Tsuda K and Tanaka M 1994 *Phil. Mag. Lett.* **70** 169
[17] Bae D H, Kim S H, Kim D H and Kim W T 2002 *Acta Mater.* **50** 2343
[18] Dubois J M, Plaindoux P, Belin-Ferre E, Tamura N and Sordelet D J 1997 *Proc. 6th Int. Conf. on Quasicrystals* (Singapore: World Scientific) p 773
[19] Singh A and Tsai A P 2008 *J. Phys.: Condens. Matter* **20**
[20] Singh A, Divakar R, Raghunathan V S, Guo J Q and Tsai A P 2002 *J. Alloys Compounds* **342** 261